

Hormone-sensitive lipase preferentially redistributes to lipid droplets associated with perilipin-5 in human skeletal muscle during moderate-intensity exercise

Katie L. Whytock , Sam O. Shepherd , Anton J. M. Wagenmakers  and Juliette A. Strauss 

Research Institute for Sport and Exercise Science, Liverpool John Moores University, Liverpool L3 3AF, UK

Edited by: Michael Hogan & Paul Greenhaff

Key points

- Hormone-sensitive lipase (HSL) and adipose triglyceride lipase (ATGL) are the key enzymes involved in intramuscular triglyceride (IMTG) lipolysis.
- In isolated rat skeletal muscle, HSL translocates to IMTG-containing lipid droplets (LDs) following electrical stimulation, but whether HSL translocation occurs in human skeletal muscle during moderate-intensity exercise is currently unknown.
- Perilipin-2 (PLIN2) and perilipin-5 (PLIN5) proteins have been implicated in regulating IMTG lipolysis by interacting with HSL and ATGL in cell culture and rat skeletal muscle studies.
- This study investigated the hypothesis that HSL (but not ATGL) redistributes to LDs during moderate-intensity exercise in human skeletal muscle, and whether the localisation of these lipases with LDs was affected by the presence of PLIN proteins on the LDs.
- HSL preferentially redistributed to PLIN5-associated LDs whereas ATGL distribution was not altered with exercise; this is the first study to illustrate the pivotal step of HSL redistribution to PLIN5-associated LDs following moderate-intensity exercise in human skeletal muscle.

Abstract Hormone-sensitive lipase (HSL) and adipose triglyceride lipase (ATGL) control skeletal muscle lipolysis. ATGL is present on the surface of lipid droplets (LDs) containing intramuscular triglyceride (IMTG) in both the basal state and during exercise. HSL translocates to LD in *ex vivo* electrically stimulated rat skeletal muscle. Perilipin-2- and perilipin-5-associated lipid droplets (PLIN2+ and PLIN5+ LDs) are preferentially depleted during exercise in humans, indicating that these PLINs may control muscle lipolysis. We aimed to test the hypothesis that in human skeletal muscle *in vivo* HSL (but not ATGL) is redistributed to PLIN2+ and PLIN5+ LDs during moderate-intensity exercise. Muscle biopsies from 8 lean trained males (age 21 ± 1 years, BMI 22.6 ± 1.2 kg m⁻² and $\dot{V}O_{2\text{peak}}$ 48.2 ± 5.0 ml min⁻¹ kg⁻¹) were obtained before and immediately following 60 min of cycling exercise at $\sim 59\%$ $\dot{V}O_{2\text{peak}}$. Cryosections were stained using antibodies targeting ATGL, HSL, PLIN2 and PLIN5. LDs were stained using BODIPY 493/503. Images

Katie Whytock is a PhD student at the Research Institute of Sport and Exercise Science at Liverpool John Moores University. Her research mainly focuses on the effects of exercise and nutrition on skeletal muscle lipid metabolism and how this links to skeletal muscle insulin resistance. She has a particular interest in the proteins associated with skeletal muscle lipid droplets and how they influence storage and utilisation of intramuscular triglyceride stores.



were obtained using confocal immunofluorescence microscopy and object-based colocalisation analyses were performed. Following exercise, HSL colocalisation to LDs increased ($P < 0.05$), and was significantly greater to PLIN5+ LDs (+53%) than to PLIN5- LDs (+34%) ($P < 0.05$), while the increases in HSL colocalisation to PLIN2+ LDs (+16%) and PLIN2- LDs (+28%) were not significantly different. Following exercise, the fraction of LDs colocalised with ATGL (0.53 ± 0.04) did not significantly change ($P < 0.05$) and was not affected by PLIN association to the LDs. This study presents the first evidence of exercise-induced HSL redistribution to LDs in human skeletal muscle and identifies PLIN5 as a facilitator of this mechanism.

(Received 30 October 2017; accepted after revision 21 February 2018; first published online 11 March 2018)

Corresponding author J. A. Strauss: Research Institute for Sport and Exercise Science, Liverpool John Moores University, Liverpool L3 3AF, UK. Email: j.a.strauss@ljmu.ac.uk

Introduction

Intramuscular triglyceride (IMTG) stores provide a readily available source of energy during moderate-intensity exercise in healthy individuals. IMTGs are stored within lipid droplets (LDs) that are located in close proximity to mitochondria (Shaw *et al.* 2008), which is believed to enable fatty acids (FAs) liberated from IMTG to be efficiently shuttled to mitochondria to produce energy. Previously there was some debate as to whether IMTG was used during exercise because the presence of extramyocellular lipid deposits in muscle samples confounded measures of net changes in IMTG content in response to exercise (Watt *et al.* 2002). Recent developments in confocal immunofluorescence microscopy have enabled the exclusion of extramyocellular lipid deposits and also permit fibre type-specific analyses to be performed. Using this approach, it is now well-established that IMTG stores are preferentially used from type I fibres in endurance-trained individuals during moderate-intensity exercise (van Loon *et al.* 2003a; Shepherd *et al.* 2013).

Hormone-sensitive lipase (HSL) was previously believed to be the only rate-limiting enzyme responsible for triacylglycerol (TAG) lipolysis (Zechner *et al.* 2009). However, it was shown that mice deficient in HSL accumulated diacylglycerol (DAG) in muscle and other tissues in response to fasting (Haemmerle *et al.* 2002), suggesting that other lipases must exist. Adipose triglyceride lipase (ATGL) was subsequently identified as a novel lipase which preferentially hydrolyses TAG (Zimmermann *et al.* 2004). Moreover, overexpression of ATGL in human primary myotubes results in reduced TAG content and increased FA release and oxidation (Badin *et al.* 2011), whilst ATGL-knockout (KO) mice accumulate TAG in skeletal muscle (Haemmerle *et al.* 2006). A pertinent role for ATGL in IMTG hydrolysis stems from the finding that IMTG breakdown still occurs in electrically stimulated rat muscle following acute pharmacological

inhibition of HSL or in muscle of HSL-KO mice (Alsted *et al.* 2013). Conversely, impairment of IMTG lipolysis during exercise in mice with muscle specific deletion of ATGL was not profound enough to impact on submaximal or maximal exercise performance, which may be due to a compensatory increase in HSL-mediated TAG hydrolysis (Dube *et al.* 2015). Together, these data suggest that both ATGL and HSL mediate IMTG hydrolysis and both can compensate functionally when the other is absent. Muscle TAG and DAG accumulate in ATGL-KO and HSL-KO mice, respectively (Haemmerle *et al.* 2002, 2006). This, in addition to HSL having a higher specificity for DAG as a substrate in comparison to TAG (Fredrikson *et al.* 1981), has led to the suggestion that ATGL and HSL hydrolyse IMTG in a sequential process in skeletal muscle. Importantly, ATGL and HSL together account for ~98% of contraction-induced TAG lipase activity in rat skeletal muscle (Alsted *et al.* 2013).

HSL activity in skeletal muscle is increased during moderate-intensity exercise through protein phosphorylation induced by contraction and adrenergic signalling mechanisms (Watt *et al.* 2003, 2006). In addition to regulation of HSL via phosphorylation, Prats *et al.* (2006) elegantly demonstrated, using confocal immunofluorescence microscopy, that HSL translocates to LDs in rat skeletal muscle *ex vivo* following stimulation with adrenaline or during electrically-induced muscle contractions. Additional examination using immunogold transmission electron microscopy on single rat muscle fibres also generated images evidencing HSL accumulation beneath the LD phospholipid monolayer, suggesting that once HSL translocates to the LDs it subsequently penetrates the phospholipid monolayer to access IMTG (Prats *et al.* 2006). Moreover, in this study the colocalisation of HSL to the LD-associated protein perilipin-2 (PLIN2) increased in response to both stimuli, implicating PLIN2 in the regulation of HSL translocation to the LDs (Prats *et al.* 2006). This was the first study to generate evidence of HSL translocation in response

to lipolytic stimuli. It is yet to be determined, however, if a similar mechanism occurs in human skeletal muscle within an *in vivo* environment where the regulation of HSL activity is under the control of multiple regulatory signalling factors that cannot be replicated *ex vivo*.

Under resting conditions, a proportion of ATGL localizes to LDs in human skeletal muscle, and this relationship is unaltered by moderate-intensity exercise (Mason *et al.* 2014). It is therefore reasonable to postulate that ATGL is regulated on the LD surface by its co-activator protein, CGI-58 (Lass *et al.* 2006). Indeed, electrical stimulation of rat skeletal muscle *ex vivo* augments the co-immunoprecipitation of ATGL and CGI-58 (MacPherson *et al.* 2013). The PLIN proteins are also believed to play a key regulatory role in controlling IMTG breakdown. Notably, the only member of the PLIN protein family that can bind ATGL is PLIN5, and in cells expressing PLIN5 both ATGL and CGI-58 are recruited to the LDs under basal conditions (Wang *et al.* 2011), suggesting that PLIN5 plays an important role in determining the activity of ATGL. Although the majority of the available evidence from cell culture studies suggests that PLIN5 (and the other PLIN proteins) facilitate the storage of TAG under basal conditions (Listenberger *et al.* 2007; Wang *et al.* 2011; Laurens *et al.* 2016), PLIN5 has also been shown to promote TAG hydrolysis under conditions stimulating lipolysis in cultured cells (Wang *et al.* 2011). Furthermore, we previously reported that LDs associated with PLIN2 or PLIN5 are preferentially utilised during 1 hour of moderate-intensity exercise (Shepherd *et al.* 2012, 2013). Whether ATGL localises to those LDs with PLIN5 associated and therefore facilitate their preferential use during exercise is yet to be investigated.

Using confocal immunofluorescence microscopy, we have previously developed methods to identify LDs with or without associated PLIN (PLIN+ LDs or PLIN- LDs, respectively; Shepherd *et al.* 2012, 2013). The aim of the present study was to extend these methods and investigate the localisation of the key lipolytic enzymes ATGL and HSL with LDs associated with PLIN2 and PLIN5 under resting conditions and in response to an acute bout of exercise in trained human skeletal muscle. We hypothesised that exercise would lead to an increase in HSL colocalisation to LDs, and that these LDs would have PLIN2 or PLIN5 associated. We also hypothesised that ATGL would already be colocalised to LDs and these LDs would be associated with PLIN5.

Methods

Participants and ethical approval

Archived muscle samples from a prior study in our laboratory comparing the effects of sprint interval and endurance training on IMTG utilisation during exercise

Table 1. Subject characteristics

Age (years)	21 ± 1
Height (m)	1.77 ± 0.03
Body mass (kg)	70.8 ± 4.5
BMI (kg m ⁻²)	22.6 ± 1.2
$\dot{V}_{O_{2peak}}$ (L min ⁻¹)	3.40 ± 0.38
$\dot{V}_{O_{2peak}}$ (ml min ⁻¹ kg ⁻¹)	48.2 ± 5.0
W_{max} (W)	253 ± 16
FFM (kg)	51.1 ± 2.7
FM (kg)	12.2 ± 1.9
ISI-Matsuda	4.7 ± 0.7

Data provided are means ± SEM ($n = 8$). BMI, body mass index; W_{max} , maximum workload; FFM, fat-free mass; FM, fat mass; ISI, insulin sensitivity index. Data obtained from post endurance training intervention from Shepherd *et al.* (2013).

(Shepherd *et al.* 2013) were utilised in the present study. Specifically, muscle samples from 8 lean, healthy male volunteers (see Table 1 for brief subject characteristics) were analysed in the present study and the informed consent provided originally covered this subsequent use. The study was approved (09/H1202/99) by the Black Country NHS research ethics committee (West Midlands, UK) and conformed to the standards set by *Declaration of Helsinki*, except for registration in a database.

Experimental procedures

Following completion of 6 weeks endurance training (cycling at 65% $\dot{V}_{O_{2peak}}$ for 40–60 min 5 days per week (see Shepherd *et al.* 2013 for further details), participants rested for >72 h and consumed a controlled diet (50%, carbohydrate, 35% fat and 15% protein) matched to habitual caloric intake for 24 h prior to the experimental trial. Following an overnight fast (>10 h), participants performed 60 min cycling on a stationary ergometer at 50 ± 2% maximal exercise capacity (W_{max} , equating to ~59% $\dot{V}_{O_{2peak}}$ achieved post-training intervention). Expired air was collected (5 min collection period) at 15 min intervals ($t = 15, 30, 45, 60$ min), using an online gas system (Oxycon Pro, Jaeger, Germany) in order to calculate rates of carbohydrate and lipid oxidation (Table 2). Additionally, heart rate was recorded every 5 min (Table 2).

Muscle biopsies were obtained from the *m. vastus lateralis* of one leg before (0 min) and immediately after exercise (60 min). The biopsied leg was randomised to avoid any bias of dominant leg. Initially local anaesthetic (1% lidocaine; B Braun, Sheffield, UK) was injected into the skin and fascia of the muscle before two small incisions were made approximately 2 cm apart. Prior to exercise, a muscle biopsy (~100 mg) was extracted from the distal incision using the Bergström needle

Table 2. Substrate utilisation during 60 min cycling at ~60% $\dot{V}_{O_2\text{peak}}$

	15 min	30 min	45 min	60 min	Overall
Heart rate (beats min ⁻¹)	134 ± 3	139 ± 5	139 ± 4	139 ± 6	138 ± 4
Percentage of $\dot{V}_{O_2\text{peak}}$	58 ± 2	59 ± 2	60 ± 2	58 ± 2	59 ± 2
RER	0.88 ± 0.01	0.86 ± 0.01	0.86 ± 0.01	0.85 ± 0.01	0.86 ± 0.01
CHO oxidation (g min ⁻¹)	1.48 ± 0.08	1.38 ± 0.08	1.36 ± 0.1	1.26 ± 0.09	1.37 ± 0.07
(% total oxidation)	61.7 ± 3.4	57.2 ± 3.6	23.34 ± 1.8	52.8 ± 4.2	56.6 ± 3.1
Fat oxidation (g min ⁻¹)	0.43 ± 0.05	0.49 ± 0.06	0.52 ± 0.05	0.54 ± 0.07	0.49 ± 0.05
(% total oxidation)	40.1 ± 3.3	44.5 ± 3.5	47 ± 3.12	48.9 ± 4.1	45.1 ± 3.1

Data provided are means ± SEM ($n = 8$). CHO, carbohydrate; RER, respiratory exchange ratio. Data obtained from Shepherd *et al.* (2013).

technique (Bergström, 1975). The muscle biopsy was first dissected from any fat or connective tissue. A portion (~60 mg) of muscle was immediately embedded in Tissue-Tek OCT compound (Sakura Finetek Europe, The Netherlands) and frozen in liquid nitrogen-cooled isopentane for subsequent immunohistochemical analyses. Following exercise, the second muscle biopsy was taken from the proximal incision using the method described above.

Analysis of muscle samples

Immunofluorescence staining. Cryosections (5 μm) were cut at -25°C onto ethanol-cleaned glass slides. Cryosections of both pre- and post-exercise samples from one participant were placed on a single slide to account for any variation in staining intensity between sections. Sections were fixed for 1 h in 3.7% formaldehyde, rinsed 3×30 s in doubly distilled water (dd H_2O) and permeabilised in 0.5% Triton X-100 for 5 min, before being washed 3×5 min in phosphate buffered saline (PBS, 137 mM sodium chloride, 3 mM potassium chloride, 8 mM sodium phosphate dibasic and 3 mM potassium phosphate monobasic, pH of 7.4). Subsequently, slides were incubated with primary antibodies (overnight for HSL analysis, 1 h for ATGL analysis) before being washed again 3×5 min in PBS. Sections were then incubated with complementary secondary fluorescence-conjugated antibodies for 30 min, followed by a further 3×5 min PBS washes. To visualise LDs, sections were incubated with BODIPY 493/503 (Invitrogen, Paisley, UK, D3922, dilution 1:50) for 20 min followed by a further 1×5 min PBS wash. After the final wash, coverslips were mounted with Vectashield (H-1000, Vector Laboratories, Burlingame, CA, USA) and sealed.

HSL and ATGL visualisation was achieved using rabbit polyclonal anti-HSL (Abcam, Cambridge, UK, ab 63492, dilution 1:50) or rabbit polyclonal anti-ATGL (Abcam, Ab109251, dilution 1:50), respectively, followed

by application of Alexa Fluor goat anti-rabbit IgG 546 secondary antibody (Invitrogen, Paisley, UK, A-11035, dilution 1:100). PLIN2 was visualised with mouse monoclonal anti-adipophilin (PLIN2) (American Research Products, MA, USA, GP40, dilution 1:50) and Alexa Fluor goat anti-mouse IgG₁ 633 secondary antibody (Invitrogen, A-21126, dilution 1:100). PLIN5 was visualised with guinea-pig polyclonal anti-OXPAT (PLIN5) (Progen Biotechnik, Germany, GP31, dilution 1:100) and Alexa Fluor goat anti-guinea-pig IgG 633 secondary antibody (Invitrogen, A-21105, dilution 1:100). Initially, sections were co-stained for HSL and LDs to investigate HSL localisation to LDs. HSL and LDs were then co-stained with either PLIN2 or PLIN5 in order to determine HSL localisation to LDs either associated (PLIN+ LDs) or not associated with each PLIN protein (PLIN- LDs). This process was then repeated with ATGL and LDs being co-stained with either PLIN2 or PLIN5 to establish ATGL localisation to LDs either associated (PLIN+ LDs) or not associated with each PLIN protein (PLIN- LDs). As described previously (Shepherd *et al.* 2012, 2013, 2017; Strauss *et al.* 2016), before any colocalisation analysis was undertaken controls were included to confirm absence of (1) bleed through of fluorophores in opposing channels when single staining was performed, (2) non-specific secondary antibody binding, and (3) sample auto-fluorescence.

Image capture, processing and data analysis. An inverted confocal microscope (Zeiss LSM710; Oberkochen, Germany) was used to obtain digital images of cross-sectionally orientated muscle sections. An argon laser was used to excite the Alexa Fluor 488 fluorophore whilst a helium-neon laser excited the Alexa Fluor 546 and 633 fluorophores. Images were initially acquired with a 40×0.7 NA oil immersion objective to examine the cellular distribution of HSL and LDs. The same system was used but with a $16 \times$ digital magnification to acquire images that were used to investigate HSL

and LDs colocalisation. A more powerful oil immersion objective of 63×1.4 NA combined with $16\times$ digital magnification was then used to identify LDs that were coated with PLIN and assess the localisation of HSL to these LDs. ATGL appeared punctate and dispersed throughout the cell and to capture its distribution more representatively, images were acquired using the 63×1.4 NA objective at a wider $8\times$ digital magnification. We were unable to stain for and identify type I fibres during the immunohistochemical analysis in the current study due to limitations on the number of fluorophores that could be used simultaneously. Instead, only muscle fibres that had the highest lipid content were imaged. Type I fibres typically have a high IMTG content alongside a large oxidative capacity (Shaw *et al.* 2008; Shepherd *et al.* 2013), and we have previously shown that IMTG utilisation during exercise occurs specifically in type I fibres (Shepherd *et al.* 2012, 2013). Results from our previous study also clearly demonstrated that in comparison to type IIa fibres, type I fibres had 3- to 4-fold and 2- to 3-fold greater IMTG stores pre and post exercise, respectively (Shepherd *et al.* 2013). Therefore, by selecting fibres with the highest lipid content we are assuming those fibres would also have the highest oxidative capacity and rates of IMTG utilisation during exercise. We expect that this approach would consequently detect changes in lipase association with LDs, if they existed. For each participant, images were obtained of pre-exercise muscle fibres ($n = 15$) and post-exercise muscle fibres ($n = 15$), with the central region of the fibre imaged for each staining combination. Due to insufficient sample being available, ATGL immunohistochemical analysis was only performed on 7 participants.

Image analysis was undertaken using Image-Pro Plus 5.1 software (Media Cybernetics, Bethesda, MD, USA). For colocalisation analysis, an intensity threshold was selected to denote the positive signal for HSL or ATGL, LDs (Fig. 1) and PLIN2 or PLIN5. These thresholds were then used to produce binary images of HSL or ATGL, LDs, and PLIN2 or PLIN5 that were subsequently used for colocalisation analysis (Fig. 1). A co-localisation map displaying the merged images was generated, and the overlapping regions extracted to a separate image. Initially colocalisation between LDs and HSL was measured by expressing the total number of extracted objects as a proportion of the total number of LDs. To determine HSL colocalisation to LDs with or without associated PLIN, the following analysis was conducted. LDs that colocalised with PLIN were first characterised as PLIN+ and PLIN- LDs (Shepherd *et al.* 2013). The number of PLIN+ LDs and PLIN- LDs that overlapped with HSL was then counted per image pre and post exercise. The number of PLIN+ and PLIN- LDs colocalised with HSL was then expressed relative to area, thereby enabling us to quantify the density of each LD subgroup to be colocalised

with HSL. HSL colocalisation to PLIN2 or PLIN5 was also quantified irrespective of LD presence. The same process was then repeated for ATGL instead of HSL. Additional analysis on the size and number of HSL or ATGL objects per image was conducted to generate a clear understanding of HSL and ATGL distribution pre and post exercise.

Statistics

All data are expressed as means \pm SEM. Significance was set at $P < 0.05$. A Student's paired *t* test was used to measure differences between pre- and post-exercise variables relating to HSL or ATGL colocalisation to LDs. A Wilcoxon signed rank test was used to measure the difference between HSL average area due to non-normally distributed data. A two-way within-subjects ANOVA was used to measure the difference between pre- and post-exercise HSL colocalisation with LDs, where within-subjects factors were identified as 'time' (pre- vs. post-exercise) and 'HSL colocalisation' (HSL+ LDs vs. HSL- LDs). A two-way within-subjects ANOVA was also used to measure the differences between pre- and post-exercise HSL or ATGL colocalisation to PLIN+ and PLIN- LDs. Here, the within-subject factors were identified as 'time' (pre- vs. post-exercise) and 'PLIN association' (PLIN+ LDs vs. PLIN- LDs). Significant main effects or interaction effects were assessed using Bonferroni adjustment *post hoc* analysis.

Results

Substrate utilisation

The respiratory exchange ratio (RER) remained stable during the 60 min of cycling at $59 \pm 2\%$ $\dot{V}_{O_{2peak}}$. Fat oxidation rates increased throughout the exercise bout and averaged $45 \pm 3\%$ of total substrate oxidation (Table 2).

Increased HSL localisation to LDs following exercise

Images of immunofluorescence staining of HSL showed large storage clusters dispersed throughout the cell (Fig. 2A). Fibres that exhibited a high lipid content were selected and images of HSL and BODIPY 493/503 were obtained from the central part of each fibre at $16\times$ digital magnification. Using this approach, it became clear that in response to exercise there was a shift in the distribution of HSL from large clusters to a greater number of smaller, discrete clusters (representative images shown in Fig. 2B). Accordingly, there was a significant increase in the number of HSL clusters after exercise (pre-exercise $0.0919 \pm 0.0068 \mu\text{m}^{-2}$; post-exercise $0.1250 \pm 0.0082 \mu\text{m}^{-2}$; $P = 0.001$) whilst the size of each HSL cluster significantly decreased (pre-exercise median = 44.20; post-exercise median = 38.04; $Z = 2.4$;

$P = 0.025$). Importantly, HSL protein content as measured by fluorescence intensity did not change with exercise (pre-exercise 39 ± 3 AU; post-exercise 42 ± 4 AU; $P = 0.107$). The fraction of LDs colocalised with HSL clusters significantly increased with exercise (19%; $P = 0.014$; Fig. 3A). At baseline, there were significantly more LDs that were colocalised to HSL than LDs without HSL colocalisation ($P = 0.033$; Fig. 3B). Following exercise there was a significant interaction effect ($P = 0.014$), the number of LDs that were colocalised to HSL significantly increased post exercise (+21%, $P = 0.014$) whereas the number of LDs without HSL colocalisation showed a trend towards a decrease post exercise (-22%, $P = 0.063$; Fig. 3B).

ATGL and LD analysis

Immunofluorescence staining of ATGL showed a distinct punctate pattern throughout the cytosol which was unaltered following exercise (Fig. 4). ATGL protein content as measured by fluorescence intensity was not significantly different after exercise (pre-exercise 7 ± 1 AU; post-exercise 8 ± 1 AU; $P = 0.354$). The average area of each ATGL object per image was unchanged (pre-exercise $40.61 \pm 8.72 \mu\text{m}^{-2}$; post-exercise $41.35 \pm 9.66 \mu\text{m}^{-2}$, $P = 0.733$). The number of ATGL objects was also unchanged (pre-exercise $0.044 \pm 0.004 \mu\text{m}^{-2}$; post-exercise $0.044 \pm 0.002 \mu\text{m}^{-2}$; $P = 0.925$). The fraction of LDs colocalised with ATGL was not significantly different after exercise (pre-exercise 0.53 ± 0.04 ; post-exercise 0.43 ± 0.05 , $P = 0.069$). Therefore, the number of LDs colocalised with ATGL was not different (pre-exercise $0.0331 \pm 0.0035 \mu\text{m}^{-2}$; post-exercise $0.0285 \pm 0.0040 \mu\text{m}^{-2}$; $P = 0.326$), and similarly, the number of LDs without ATGL colocalisation

was not different (pre-exercise $0.0304 \pm 0.0028 \mu\text{m}^{-2}$; post-exercise $0.0350 \pm 0.0021 \mu\text{m}^{-2}$; $P = 0.253$).

Relationship between HSL, PLIN2 or PLIN5 and LDs

To quantify colocalisation between HSL and PLIN2+ LDs or PLIN2- LDs, images of HSL, PLIN2 and LDs were acquired pre and post exercise at $16\times$ magnification using a 63×1.4 NA objective (Fig. 5A). This process was then repeated for HSL, PLIN5 and LDs (Fig. 5B). The number of HSL objects colocalised to PLIN2 increased after exercise (pre-exercise $0.0688 \pm 0.0030 \mu\text{m}^{-2}$; post-exercise $0.0773 \pm 0.0020 \mu\text{m}^{-2}$; $P = 0.049$). However, not all LDs have PLIN2 bound to them, and therefore we investigated the colocalisation of HSL with PLIN2+ and PLIN2- LDs. Pre-exercise, the number of PLIN2+ LDs colocalised to HSL was greater ($0.0565 \pm 0.0043 \mu\text{m}^{-2}$) than the number of PLIN2- LDs not colocalised with HSL ($0.0205 \pm 0.0019 \mu\text{m}^{-2}$; $P < 0.001$; Fig. 6A). Exercise led to an increase in HSL colocalisation to both PLIN2+ LDs (+16%) and PLIN2- LDs (+28%; Fig. 6A, $P = 0.047$) post exercise. There was however, no interaction effect for exercise and PLIN2 presence on the LDs ($P = 0.611$).

The number of HSL objects colocalised to PLIN5 also increased after exercise (pre-exercise $0.0573 \pm 0.0043 \mu\text{m}^{-2}$; post-exercise $0.0772 \pm 0.0056 \mu\text{m}^{-2}$; $P = 0.002$). Before exercise, the number of PLIN5+ LDs colocalised with HSL was greater ($0.0406 \pm 0.0043 \mu\text{m}^{-2}$) than the number of PLIN5- LDs without HSL colocalisation ($0.0149 \pm 0.0015 \mu\text{m}^{-2}$; $P = 0.001$; Fig. 6B). There was a main effect for exercise on HSL colocalisation to LDs ($P < 0.001$; Fig. 6B), such that HSL colocalisation to LDs increased. Moreover, there was a significant interaction effect for exercise and PLIN5 presence on the LDs. The increase in HSL colocalisation to PLIN5+ LDs

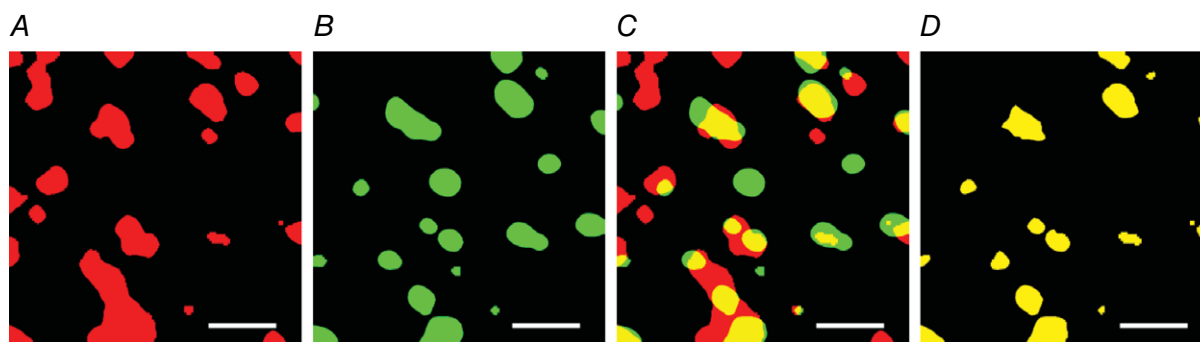


Figure 1. Method of colocalisation analysis

Binary images of objects representing HSL (A) and LDs (B) identified by a selected intensity threshold to signify a positive signal for HSL or LDs, respectively. C, colocalisation of HSL objects and LDs was investigated by merging the images. D, the extracted objects represent positive colocalisation between HSL and LDs. Any LD that overlapped with a HSL object was counted as a colocalisation event. If the same HSL object overlapped more than once with a LD then this was counted as a dual colocalisation event and omitted from the analysis, allowing for only one colocalisation event to be counted. The same procedure was used to obtain colocalisation analysis for ATGL objects and LDs, and PLIN2 or PLIN5 and LDs. Scale bars represent $3 \mu\text{m}$. [Colour figure can be viewed at wileyonlinelibrary.com]

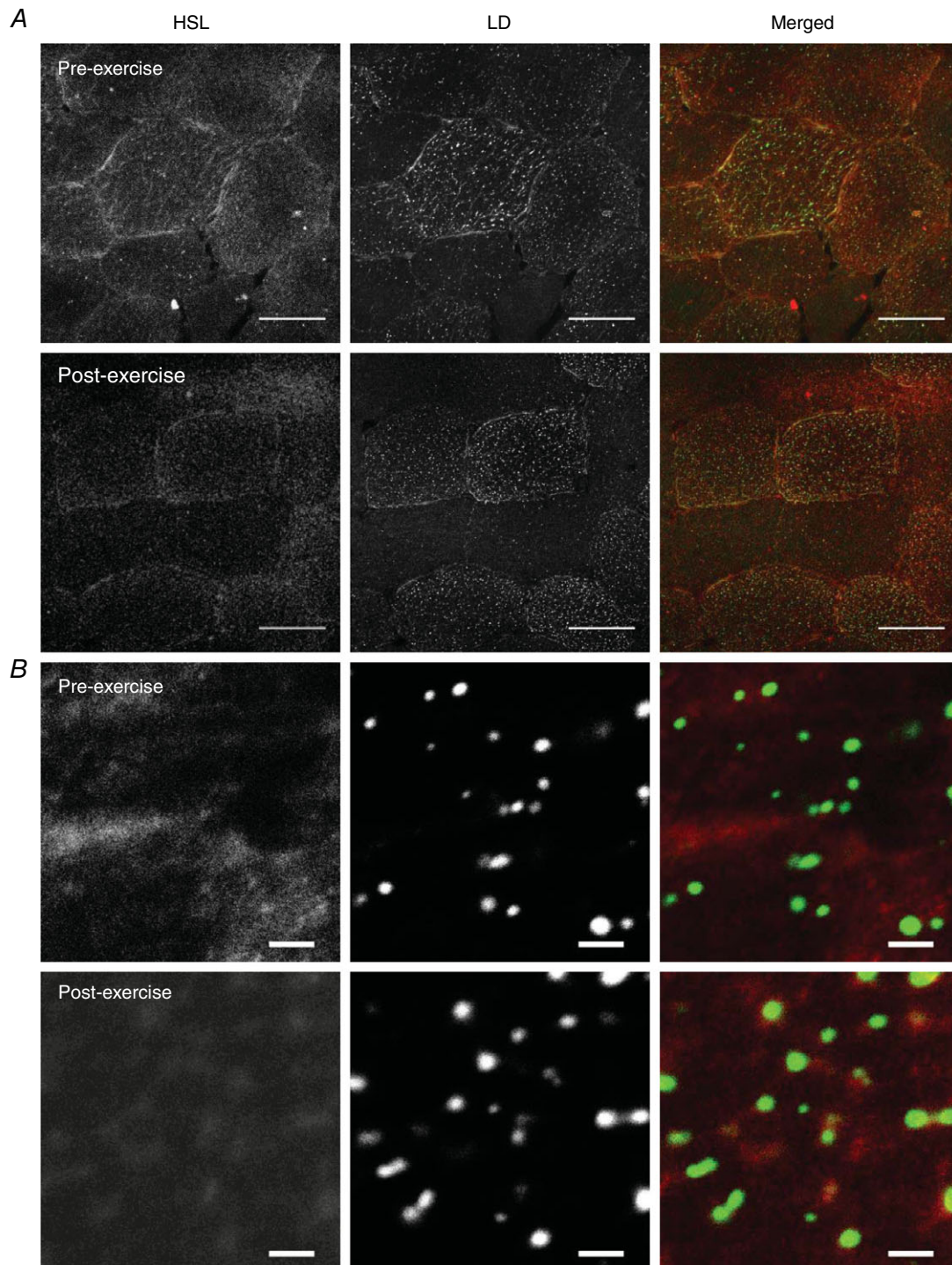


Figure 2. HSL redistributes to LDs after exercise as visualised through confocal immunofluorescence microscopy

A, representative images of HSL and LDs pre and post exercise were initially obtained using a 40 \times oil objective on a confocal microscope. Scale bars represent 50 μm . LDs were visualised using BODIPY 493/503 and represent IMTG stores within the cell. Muscle fibres that had the highest lipid droplet content were selected for analysis. *B*, a 16 \times digital magnification was then applied to the centre of these muscle fibres and images were obtained to identify and quantify distribution and colocalisation between HSL and LDs. Scale bars represent 2 μm . Panel *B* shows that in the pre-exercise state HSL appeared as large storage clusters throughout the cell, whereas post-exercise HSL was visualised as a greater number of smaller, discrete clusters centred on LDs, as observed on the merged images. [Colour figure can be viewed at wileyonlinelibrary.com]

(+53%) was greater than the increase to PLIN5- LDs (+34%; $P = 0.006$; Fig. 6B) post exercise.

Relationship between ATGL, PLIN2 or PLIN5 and LDs

To quantify colocalisation between ATGL and PLIN2+ LDs or PLIN2- LDs, $16\times$ magnification images of ATGL, PLIN2 and LDs using a 63×1.4 NA objective were acquired pre and post exercise (Fig. 4B). This process was then repeated for ATGL, PLIN5 and LDs. Before exercise, more ATGL was colocalised to PLIN2+ LDs ($0.0224 \pm 0.0029 \mu\text{m}^{-2}$) than to PLIN2- LDs ($0.0057 \pm 0.001 \mu\text{m}^{-2}$, $P < 0.001$; Fig. 7A) and this was unaltered with exercise ($P = 0.187$). Similarly, before exercise, more ATGL was colocalised to PLIN5+ LDs ($0.0222 \pm 0.0017 \mu\text{m}^{-2}$) than to PLIN5- LDs ($0.0109 \pm 0.0019 \mu\text{m}^{-2}$, $P < 0.001$; Fig. 7B) and this was also not altered with exercise ($P = 0.287$). There was no significant difference in the amount of ATGL colocalised to PLIN2 after exercise (pre-exercise $0.037 \pm 0.0033 \mu\text{m}^{-2}$; post-exercise $0.037 \pm 0.0023 \mu\text{m}^{-2}$; $P = 0.985$). There was also no significant difference in the amount of ATGL colocalised to PLIN5 (pre-exercise $0.0305 \pm 0.0018 \mu\text{m}^{-2}$; post-exercise $0.0311 \pm 0.0023 \mu\text{m}^{-2}$; $P = 0.877$).

Discussion

This study examined the localisation of the two key lipases in human skeletal muscle, ATGL and HSL, with LDs and the associated PLIN proteins at rest and in response to moderate-intensity exercise. The major novel

observation is that HSL redistributes to LDs in human skeletal muscle following 1 h of moderate-intensity cycling exercise, with HSL preferentially redistributing to LDs with associated PLIN5. Furthermore, we confirm for the first time that ATGL was colocalised more to PLIN5+ LDs than to PLIN5- LDs, in agreement with our hypothesis. Additionally, the data show that ATGL is also colocalised more to PLIN2+ LDs than to PLIN2- LDs and the distribution of ATGL does not alter during the exercise bout. Together, these data demonstrate different distribution patterns of key lipases and their localisation to LD-associated PLIN proteins in skeletal muscle, which may be important in the regulation of IMTG utilisation during moderate-intensity exercise.

In the basal state HSL was observed as large storage clusters throughout the cell, whereas after exercise HSL was visualised as a greater number of smaller, discrete clusters typically centred on LDs (Fig. 2B). As a result, we observed an increase in the fraction of LDs colocalising with HSL after exercise, demonstrating that HSL redistributes to LDs in response to exercise in human skeletal muscle. A number of studies in cultured adipocytes have demonstrated that HSL translocates from the cytosol to LDs in response to lipolytic stimuli (Su *et al.* 2003; Sztalryd *et al.* 2003; Wang *et al.* 2009), whereas studies investigating the localisation of HSL in skeletal muscle are limited. Most notably, in line with our findings, Prats *et al.* (2006), using confocal immunofluorescence microscopy and isolated rat skeletal muscle fibres, observed that HSL in the basal state was accumulating either as storage clusters or colocalising with LDs, while *ex vivo*

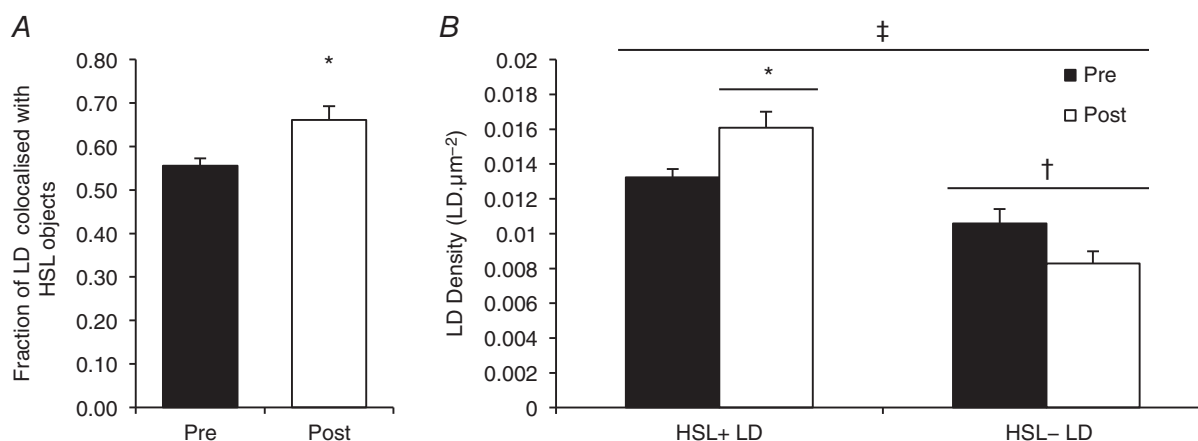


Figure 3. HSL redistributes from larger storage clusters to smaller more frequent clusters after exercise, resulting in an increase in LD colocalisation to HSL

Quantification derived from confocal immunofluorescence microscopy images. *A*, colocalisation analysis was performed to determine the fraction of LDs overlapping with HSL objects before and after exercise. *B*, subsequently, the number of LDs colocalised with HDL (HSL+ LDs) or not colocalised with HSL (HSL- LDs) was calculated and pre- and post-exercise values were compared. Data collected are averages of 15 fibres per participant per time point. Values are given as means \pm SEM ($n = 8$ per group). †Main effect for HSL colocalisation to LDs ($P < 0.05$ vs. HSL- LDs). ‡Main interaction effect for HSL colocalisation to LDs after exercise ($P < 0.05$). *Post hoc* analysis revealed an increase in HSL+ LDs ($*P < 0.05$ versus pre-exercise) and a trend towards a decrease in HSL- LDs ($P = 0.063$ versus pre-exercise).

electrical or adrenaline stimulation increased the translocation of HSL to LDs. In addition, using transmission electron microscopy with immunogold labelled HSL antibodies, Prats *et al.* (2006) showed that the HSL translocation led to HSL passing through the phospholipid monolayer of the LDs into the TAG core, allowing HSL

(the enzyme) greater access to IMTG (the substrate). The *ex vivo* protocol adopted by Prats *et al.* (2006) elegantly eliminates the interference of plasma-derived FAs on substrate use and IMTG synthesis, allowing IMTG hydrolysis to be studied in isolation. We now extend these findings to demonstrate that HSL redistribution occurs in human

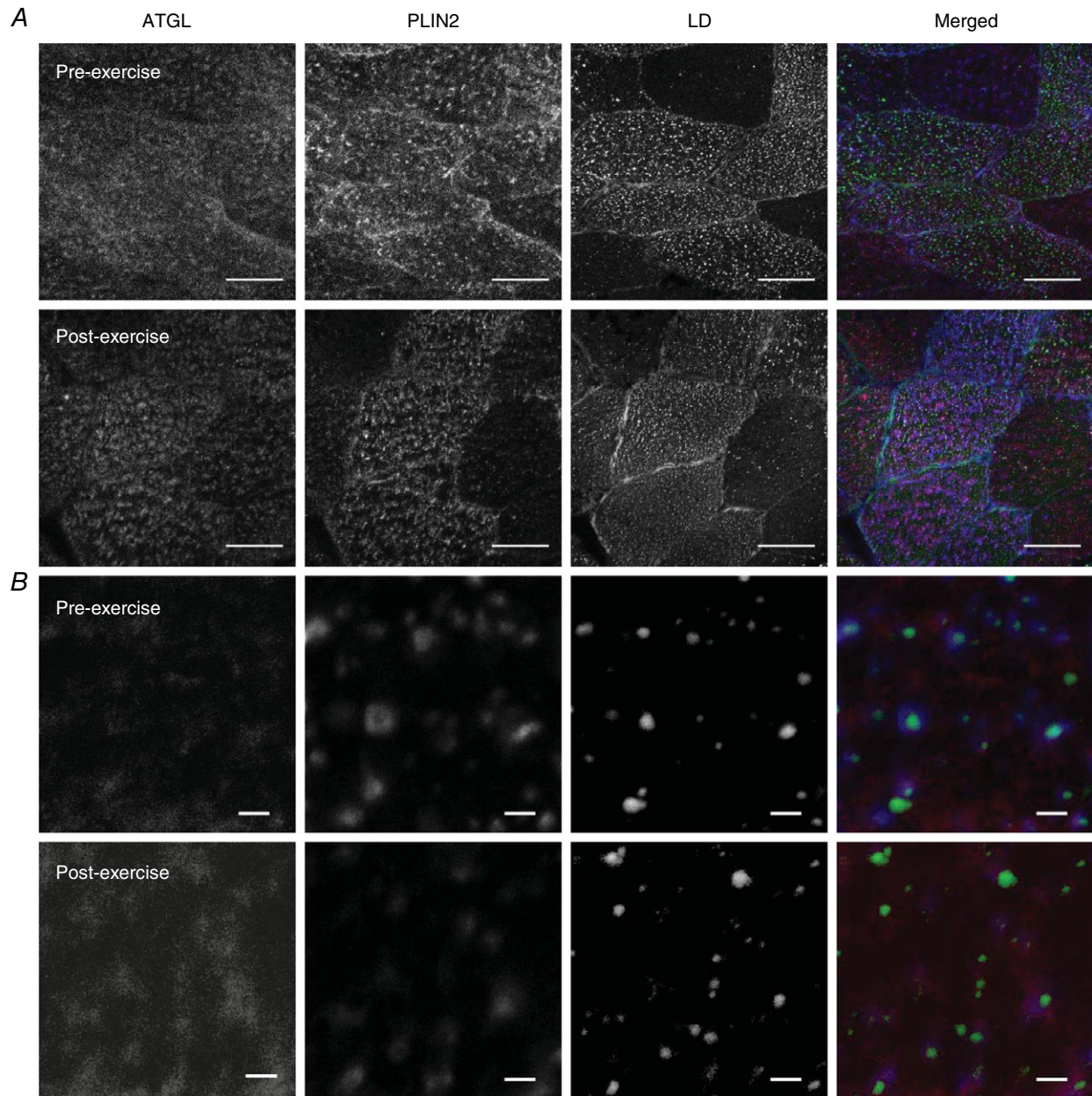


Figure 4. ATGL distribution does not change after exercise as visualised through immunofluorescence microscopy

A, representative images of ATGL, PLIN2 and LDs before and after exercise obtained using a 63× oil objective on a confocal microscope. Scale bars represent 50 μm. LDs were visualised using BODIPY 493/503 and represent IMTG stores within the cell. Muscle fibres that had the highest lipid droplet content were selected and analysed. B, an 8× digital magnification was then applied to the centre of these muscle fibres and images were obtained to identify and quantify distribution and colocalisation between ATGL and LDs associated with either PLIN2 or PLIN5 (not shown). Scale bars represent 2 μm. Panels A and B show that pre-exercise ATGL had punctate staining throughout the cell and this was unaltered post exercise. [Colour figure can be viewed at wileyonlinelibrary.com]

skeletal muscle in response to moderate-intensity exercise *in vivo*.

Overall we observed an increase in HSL colocalisation to PLIN2 and PLIN5 following exercise. This finding is in agreement with Prats *et al.* (2006), who demonstrated an increased colocalisation of HSL with PLIN2, but did not investigate PLIN5. In addition, by staining HSL, LDs and either PLIN2 or PLIN5, we were able to determine specific colocalisation between HSL and different sub-groups

of LDs (PLIN2+ LDs and PLIN2- LDs or PLIN5+ LDs and PLIN5- LDs). The most important and novel finding of the present study was that HSL preferentially redistributed to LDs with associated PLIN5. Although PLIN5 is implicated in protecting intracellular TAG stores from hydrolysis under basal conditions (Wang *et al.* 2011; Laurens *et al.* 2016), evidence is accumulating that PLIN5 also facilitates TAG breakdown when energy demand increases. PLIN5 is phosphorylated in response to PKA

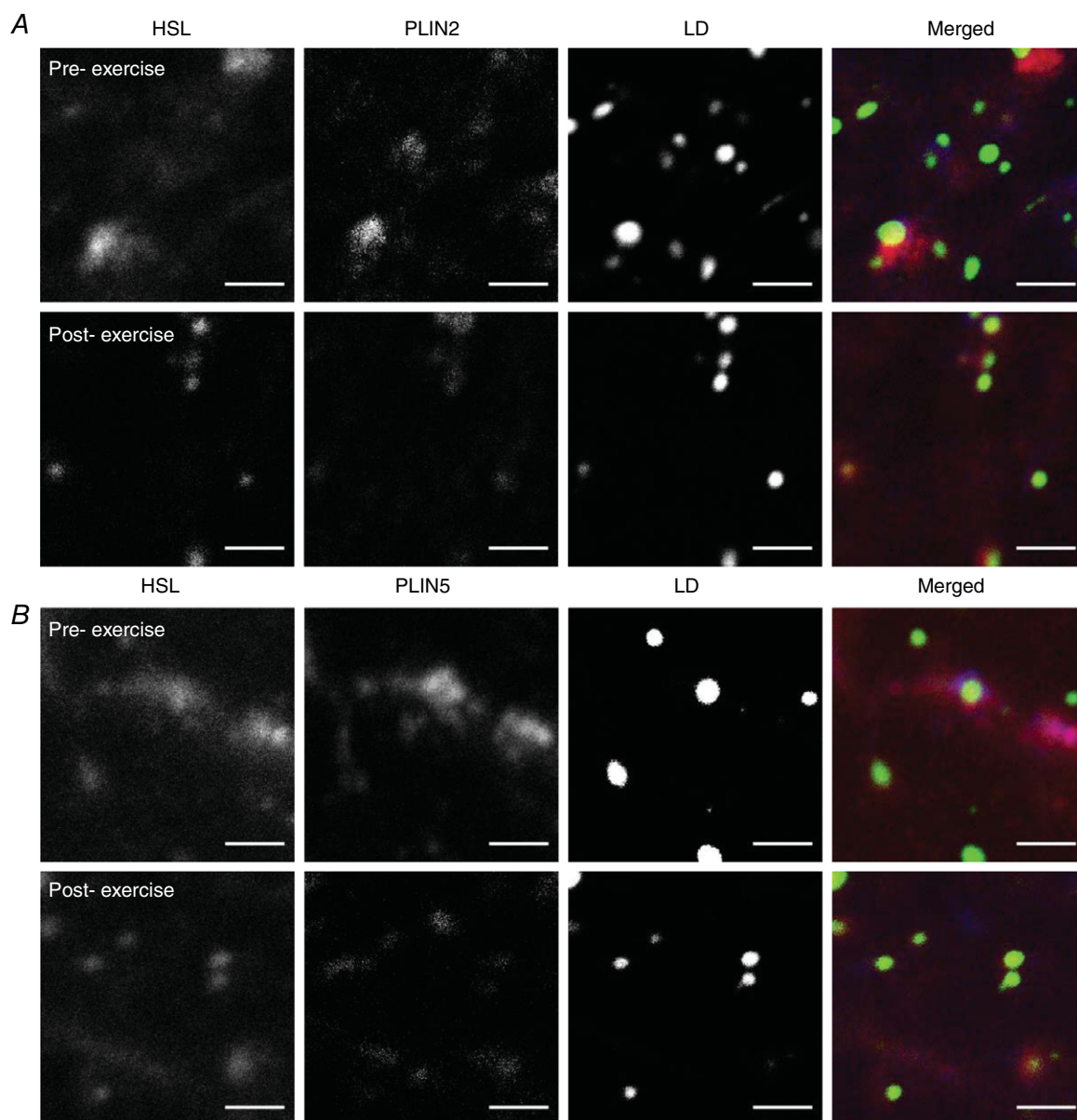


Figure 5. Immunofluorescence microscopy images of HSL, PLIN2/PLIN5 and LDs before and after exercise
Colocalisation between HSL, LDs and PLIN2 (A) or PLIN5 (B) as visualised through immunofluorescence microscopy and quantified before and after exercise. Images captured with a 63× oil objective on a confocal microscope at 16× digital magnification in the central region of fibres that had the highest lipid droplet content. Scale bars represent 2 μm. PLIN2 (A) and PLIN5 (B) were associated with LDs or located in the cytosol. HSL redistributes from larger storage clusters to a greater number of smaller, discrete clusters centred on different subclasses of LDs (i.e. PLIN+ or PLIN- LDs). [Colour figure can be viewed at wileyonlinelibrary.com]

stimulation, leading to TAG hydrolysis in cultured cells (Wang *et al.* 2011). In addition, we have previously shown that LDs with associated PLIN5 are preferentially used during a bout of moderate-intensity exercise in lean, healthy individuals (Shepherd *et al.* 2013). We now propose that PLIN5+ LDs are targeted for breakdown during exercise because PLIN5 facilitates the interaction of HSL with the TAGs stored in the LD core.

Immunofluorescence staining of ATGL displayed a punctate pattern throughout the cytosol which was not altered in response to moderate-intensity exercise (Fig. 4). At baseline, the fraction of LDs colocalising with ATGL was ~0.53 and this was not altered following exercise. Mason *et al.* (2014) recently reported no significant changes in the percentage of ATGL colocalising with LDs (stained using Oil Red O) in human skeletal muscle of

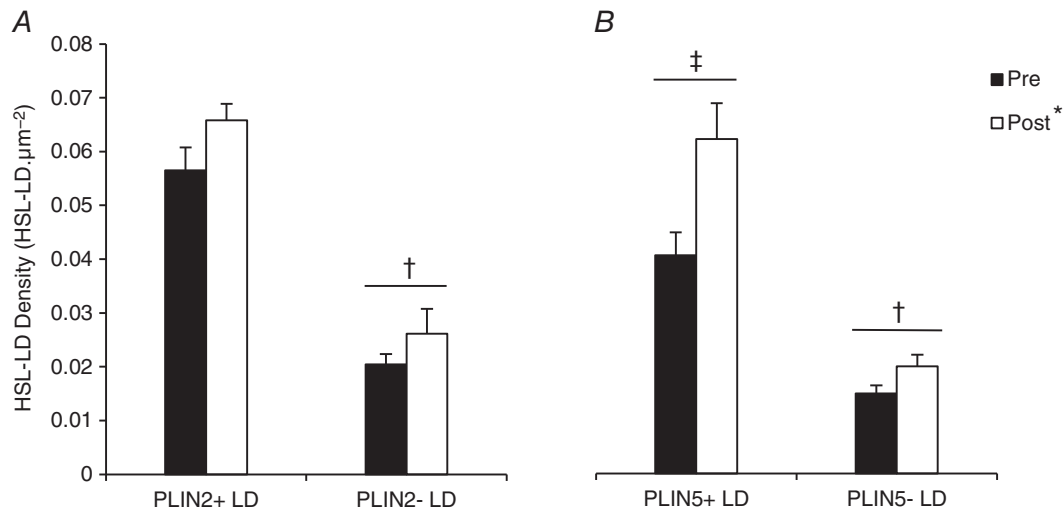


Figure 6. HSL preferentially redistributes to PLIN5+ LDs after exercise

HSL colocalisation with different LDs pools (PLIN+ or PLIN- LDs) was quantified from immunofluorescence microscopy images of HSL, LDs and PLIN2 (A) or PLIN5 (B) before and after exercise. Data were collected as averages of 15 fibres per participant per time point. Values are presented as means \pm SEM ($n = 8$ per group). *Main effect for exercise ($P < 0.05$ vs. pre-exercise). †Main effect for PLIN association with LDs ($P < 0.05$ vs. PLIN- LDs). ‡Main interaction effect for PLIN5 association with LDs ($P < 0.05$ vs. PLIN- LDs).

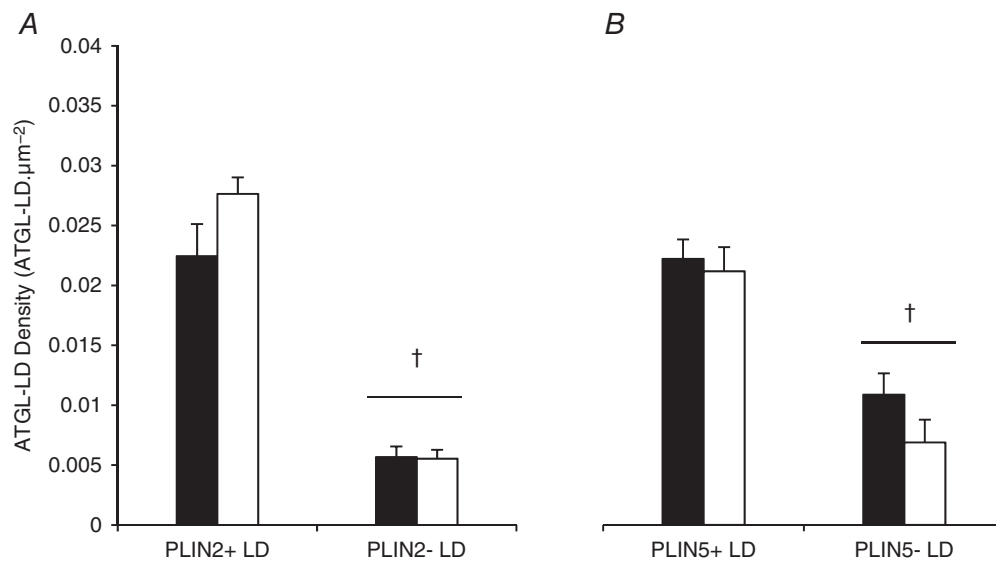


Figure 7. ATGL colocalisation with different pools of LDs does not change after exercise

ATGL colocalisation with different LDs pools (PLIN+ or PLIN- LDs) was quantified from immunofluorescence microscopy images of ATGL, LDs and PLIN2 (A) or PLIN5 (B) before and after exercise. Data were collected as averages of 15 fibres per participant per time point. Values are presented as means \pm SEM ($n = 7$ per group). †Main effect for PLIN association with LDs ($P < 0.05$ vs. PLIN- LDs).

recreationally active males following moderate-intensity exercise. Together these results suggest that a proportion of LDs are already colocalising with ATGL under basal conditions and the activity of ATGL is regulated locally by its co-activator CGI-58 rather than any redistribution of ATGL. In line with this suggestion, studies in cultured COS-7 cells have shown that overexpression of CGI-58 led to an increase in ATGL activity (Lass *et al.* 2006). The fraction of LDs colocalising with ATGL showed a trend towards a decrease after exercise, which is probably explained by a decrease in LD number post exercise (Shepherd *et al.* 2013). Interestingly the results show there is a substantial fraction of LDs (~0.47) that do not have any colocalisation with ATGL. As HSL acts both on TAG and DAG (Lass *et al.* 2011), it is plausible that LDs not colocalised with ATGL are instead subject to HSL-mediated hydrolysis.

Evidence from cultured cells suggests that PLIN5 recruits and binds ATGL and CGI-58 at the LD surface under basal conditions but releases ATGL and CGI-58 following PKA-induced phosphorylation (Granneman *et al.* 2011; Wang *et al.* 2011). The release of ATGL and CGI-58 from PLIN5 allows ATGL to bind to its co-activator CGI-58 to increase ATGL activity (Granneman *et al.* 2011; Wang *et al.* 2011). In the current study, at baseline, ATGL colocalised more to PLIN2+ LDs and PLIN5+ LDs than to PLIN2- LDs and PLIN5- LDs (Fig. 7). As ATGL distribution did not change during exercise, the amount of ATGL colocalised with PLIN2+ LDs and PLIN5+ LDs was also not altered after the exercise bout. There was also no change in ATGL colocalisation with PLIN2 or PLIN5, irrespective of LD presence following exercise. In line with our findings, MacPherson *et al.* (2013) also reported that PLIN2 and PLIN5 both co-immunoprecipitated with ATGL under basal conditions, but this did not increase in response to lipolytic stimuli (adrenaline, contraction or both) in rat skeletal muscle. Our data therefore suggest that PLIN2 and PLIN5 may support the colocalisation of ATGL to LDs during fasted, non-exercised conditions. Immunogold labelling of HSL with transmission electron microscopy has confirmed that HSL penetrates the phospholipid monolayer of the LDs to access IMTG in response to adrenaline or electrical stimulation in isolated rat skeletal muscle (Prats *et al.* 2006). Whether PLIN2 or PLIN5 first localises ATGL on the outside of the LDs phospholipid monolayer during basal conditions but then releases ATGL so it can penetrate the phospholipid monolayer and access IMTG stores clearly warrants further investigation but can only accurately be deciphered using immunogold transmission electron microscopy.

IMTG utilisation during 60 min of moderate-intensity cycling exercise in these muscle samples has been quantified previously (Shepherd *et al.* 2013), where it was confirmed that IMTG content decreased after exercise

($-43 \pm 5\%$) in type I fibres only. Due to constraints with the number of fluorophores that could be used simultaneously, we were unable to stain and identify type I fibres as part of the analysis in this study. Instead, fibres with the highest lipid content were selected for analysis. Type I fibres are characterised by high mitochondrial content and elevated IMTG stores (Shaw *et al.* 2008; Shepherd *et al.* 2013). It is well documented that IMTG utilisation is strongly associated with pre-exercise IMTG content (van Loon *et al.* 2003a, b) and it is therefore likely that the fibres selected in the current study also exhibited net IMTG breakdown. Moreover, despite being unable to identify fibre type in the current study we can conclude that redistribution of HSL occurs in fibres that have a high LD content.

By extending our validated immunofluorescence microscopy techniques, we have been able to generate further insight into the role of the PLIN proteins in the regulation of lipolysis in skeletal muscle during endurance exercise. Our assays, however, only permit the analysis of ATGL or HSL colocalisation with LDs with a single PLIN protein. It is possible, therefore, that PLIN2+ LDs or PLIN2- LDs may also have associated PLIN5 and similarly PLIN5+ LDs and PLIN5- LDs may have associated PLIN2. Nevertheless, the results indicate that whilst there were similar increases in HSL colocalisation to PLIN2+ LDs and PLIN2- LDs post exercise, there was a significantly greater increase in HSL colocalisation to PLIN5+ LDs than to PLIN5- LDs after the exercise bout. It is also possible, that PLIN5 was also present on the surface of PLIN2+ LDs or PLIN2- LDs colocalised with ATGL. Despite this limitation, we can still conclude that ATGL was present on PLIN5- LDs and therefore PLIN5 is not a prerequisite for ATGL colocalisation to the LDs.

In conclusion, this study has generated novel evidence that HSL redistributes to LDs in skeletal muscle of endurance-trained men in response to moderate-intensity exercise, whereas ATGL colocalisation with LDs is unaltered by exercise. Furthermore, this is the first study to demonstrate that HSL preferentially redistributes to PLIN5+ LDs following moderate intensity exercise, demonstrating a novel mechanism by which PLIN5 regulates HSL recruitment to LDs which could aid in subsequent IMTG utilisation during exercise.

References

- Alsted TJ, Ploug T, Prats C, Serup AK, Hoeg L, Schjerling P, Holm C, Zimmermann R, Fledelius C, Galbo H & Kiens B (2013). Contraction-induced lipolysis is not impaired by inhibition of hormone-sensitive lipase in skeletal muscle. *J Physiol* **591**, 5141–5155.
- Badin PM, Louche K, Mairal A, Liebisch G, Schmitz G, Rustan AC, Smith SR, Langin D & Moro C (2011). Altered skeletal muscle lipase expression and activity contribute to insulin resistance in humans. *Diabetes* **60**, 1734–1742.

- Bergström J (1975). Percutaneous needle biopsy of skeletal muscle in physiological and clinical research. *Scand J Clin Lab Invest* **35**, 609–616.
- Dube JJ, Sitnick MT, Schoiswohl G, Wills RC, Basantani MK, Cai L, Puliniakunnil T & Kershaw EE (2015). Adipose triglyceride lipase deletion from adipocytes, but not skeletal myocytes, impairs acute exercise performance in mice. *Am J Physiol Endocrinol Metab* **308**, E879–E890.
- Fredrikson G, Stralfors P, Nilsson NO & Belfrage P (1981). Hormone-sensitive lipase from adipose tissue of rat. *Methods Enzymol* **71**, 636–646.
- Granneman JG, Moore HP, Mottillo EP, Zhu Z & Zhou L (2011). Interactions of perilipin-5 (Plin5) with adipose triglyceride lipase. *J Biol Chem* **286**, 5126–5135.
- Haemmerle G, Lass A, Zimmermann R, Gorkiewicz G, Meyer C, Rozman J, Heldmaier G, Maier R, Theussl C, Eder S, Kratky D, Wagner EF, Klingenspor M, Hoefler G & Zechner R (2006). Defective lipolysis and altered energy metabolism in mice lacking adipose triglyceride lipase. *Science* **312**, 734–737.
- Haemmerle G, Zimmermann R, Hayn M, Theussl C, Waeg G, Wagner E, Sattler W, Magin TM, Wagner EF & Zechner R (2002). Hormone-sensitive lipase deficiency in mice causes diglyceride accumulation in adipose tissue, muscle, and testis. *J Biol Chem* **277**, 4806–4815.
- Lass A, Zimmermann R, Haemmerle G, Riederer M, Schoiswohl G, Schweiger M, Kienesberger P, Strauss JG, Gorkiewicz G & Zechner R (2006). Adipose triglyceride lipase-mediated lipolysis of cellular fat stores is activated by CGI-58 and defective in Chanarin-Dorfman Syndrome. *Cell Metab* **3**, 309–319.
- Lass A, Zimmermann R, Oberer M & Zechner R (2011). Lipolysis – a highly regulated multi-enzyme complex mediates the catabolism of cellular fat stores. *Prog Lipid Res* **50**, 14–27.
- Laurens C, Bourlier V, Mairal A, Louche K, Badin PM, Mouisel E, Montagner A, Marette A, Tremblay A, Weisnagel JS, Guillou H, Langin D, Joannisse DR & Moro C (2016). Perilipin 5 fine-tunes lipid oxidation to metabolic demand and protects against lipotoxicity in skeletal muscle. *Sci Rep* **6**, 38310.
- Listenberger LL, Ostermeyer-Fay AG, Goldberg EB, Brown WJ & Brown DA (2007). Adipocyte differentiation-related protein reduces the lipid droplet association of adipose triglyceride lipase and slows triacylglycerol turnover. *J Lipid Res* **48**, 2751–2761.
- MacPherson RE, Ramos SV, Vandenboom R, Roy BD & Peters SJ (2013). Skeletal muscle PLIN proteins, ATGL and CGI-58, interactions at rest and following stimulated contraction. *Am J Physiol Regul Integr Comp Physiol* **304**, R644–R650.
- Mason RR, Meex RC, Russell AP, Canny BJ & Watt MJ (2014). Cellular localization and associations of the major lipolytic proteins in human skeletal muscle at rest and during exercise. *PLoS One* **9**, e103062.
- Prats C, Donsmark M, Qvortrup K, Londos C, Sztalryd C, Holm C, Galbo H & Ploug T (2006). Decrease in intramuscular lipid droplets and translocation of HSL in response to muscle contraction and epinephrine. *J Lipid Res* **47**, 2392–2399.
- Shaw CS, Jones DA & Wagenmakers AJ (2008). Network distribution of mitochondria and lipid droplets in human muscle fibres. *Histochem Cell Biol* **129**, 65–72.
- Shepherd SO, Cocks M, Tipton KD, Ranasinghe AM, Barker TA, Burniston JG, Wagenmakers AJ & Shaw CS (2012). Preferential utilization of perilipin 2-associated intramuscular triglycerides during 1 h of moderate-intensity endurance-type exercise. *Exp Physiol* **97**, 970–980.
- Shepherd SO, Cocks M, Tipton KD, Ranasinghe AM, Barker TA, Burniston JG, Wagenmakers AJ & Shaw CS (2013). Sprint interval and traditional endurance training increase net intramuscular triglyceride breakdown and expression of perilipin 2 and 5. *J Physiol* **591**, 657–675.
- Shepherd SO, Strauss JA, Wang Q, Dube JJ, Goodpaster B, Mashek DG & Chow LS (2017). Training alters the distribution of perilipin proteins in muscle following acute free fatty acid exposure. *J Physiol* **595**, 5587–5601.
- Strauss JA, Shaw CS, Bradley H, Wilson OJ, Dorval T, Pilling J & Wagenmakers AJ (2016). Immunofluorescence microscopy of SNAP23 in human skeletal muscle reveals colocalization with plasma membrane, lipid droplets, and mitochondria. *Physiol Rep* **4**, e12662.
- Su CL, Sztalryd C, Contreras JA, Holm C, Kimmel AR & Londos C (2003). Mutational analysis of the hormone-sensitive lipase translocation reaction in adipocytes. *J Biol Chem* **278**, 43615–43619.
- Sztalryd C, Xu G, Dorward H, Tansey JT, Contreras JA, Kimmel AR & Londos C (2003). Perilipin A is essential for the translocation of hormone-sensitive lipase during lipolytic activation. *J Cell Biol* **161**, 1093–1103.
- van Loon LJ, Koopman R, Stegen JH, Wagenmakers AJ, Keizer HA & Saris WH (2003a). Intramyocellular lipids form an important substrate source during moderate intensity exercise in endurance-trained males in a fasted state. *J Physiol* **553**, 611–625.
- van Loon LJ, Schrauwen-Hinderling VB, Koopman R, Wagenmakers AJ, Hesselink MK, Schaart G, Kooi ME & Saris WH (2003b). Influence of prolonged endurance cycling and recovery diet on intramuscular triglyceride content in trained males. *Am J Physiol Endocrinol Metab* **285**, E804–E811.
- Wang H, Bell M, Sreenivasan U, Hu H, Liu J, Dalen K, Londos C, Yamaguchi T, Rizzo MA, Coleman R, Gong D, Brasaemle D & Sztalryd C (2011). Unique regulation of adipose triglyceride lipase (ATGL) by perilipin 5, a lipid droplet-associated protein. *J Biol Chem* **286**, 15707–15715.
- Wang H, Hu L, Dalen K, Dorward H, Marcinkiewicz A, Russell D, Gong D, Londos C, Yamaguchi T, Holm C, Rizzo MA, Brasaemle D & Sztalryd C (2009). Activation of hormone-sensitive lipase requires two steps, protein phosphorylation and binding to the PAT-1 domain of lipid droplet coat proteins. *J Biol Chem* **284**, 32116–32125.
- Watt MJ, Heigenhauser GJ & Spriet LL (2002). Intramuscular triacylglycerol utilization in human skeletal muscle during exercise: is there a controversy? *J Appl Physiol* (1985) **93**, 1185–1195.

- Watt MJ, Holmes AG, Pinnamaneni SK, Garnham AP, Steinberg GR, Kemp BE & Febbraio MA (2006). Regulation of HSL serine phosphorylation in skeletal muscle and adipose tissue. *Am J Physiol Endocrinol Metab* **290**, E500–E508.
- Watt MJ, Stellingwerff T, Heigenhauser GJ & Spriet LL (2003). Effects of plasma adrenaline on hormone-sensitive lipase at rest and during moderate exercise in human skeletal muscle. *J Physiol* **550**, 325–332.
- Zechner R, Kienesberger PC, Haemmerle G, Zimmermann R & Lass A (2009). Adipose triglyceride lipase and the lipolytic catabolism of cellular fat stores. *J Lipid Res* **50**, 3–21.
- Zimmermann R, Strauss JG, Haemmerle G, Schoiswohl G, Birner-Gruenberger R, Riederer M, Lass A, Neuberger G, Eisenhaber F, Hermetter A & Zechner R (2004). Fat mobilization in adipose tissue is promoted by adipose triglyceride lipase. *Science* **306**, 1383–1386.

Additional information

Competing interest

The authors declare that they have no competing interests.

Author contributions

K.L.W., S.O.S. and J.A.S. were responsible for the conception and design of the experiments. K.L.W., S.O.S. and J.A.S. were responsible for the collection and analysis of data. K.L.W., S.O.S., A.J.M.W. and J.A.S. were responsible for interpretation of the data and drafting and revisions of the manuscript. All authors approved of the final version of the manuscript, and agree to be accountable for all aspects of the work in ensuring that questions related to the accuracy or integrity of any part of the work are appropriately investigated and resolved, and all persons designated as authors qualify for authorship, and all those who qualify for authorship are listed.

Funding

K.L.W. is in receipt of a PhD scholarship from Liverpool John Moores University.

Acknowledgements

The muscle samples used in this study were obtained from a previous study. The authors would like to thank Dr Christopher Shaw and Dr Matthew Cocks in their assistance in collecting the original samples.